

# BEC-BCS Crossover in the $\epsilon$ Expansion

Jiunn-Wei Chen and Eiji Nakano

*Department of Physics and Center for Theoretical Sciences,  
National Taiwan University, Taipei 10617, Taiwan*

The  $\epsilon$  expansion (expansion around four spacial dimensions) developed by Nishida and Son for a cold fermi gas with infinite scattering length is extended to finite scattering length to study the BEC-BCS crossover. A resummation of higher order logarithms and a suitable extension of fermion coupling in  $d$ -dimensions are developed in order to apply the theory in the BCS regime. The ratio between the chemical potential and the Fermi energy,  $\mu/\varepsilon_F$ , is computed to next-to-leading order in the  $\epsilon$  expansion as a function of  $\eta = 1/(ak_F)$ , where  $a$  is the scattering length and  $k_F$  is the Fermi momentum in a non-interacting system. Near the unitarity limit  $|\eta| \rightarrow 0$ , we found  $\mu/\varepsilon_F = 0.475 - 0.707\eta - 0.5\eta^2$ . Near the BEC limit  $\eta \rightarrow \infty$ ,  $\mu/\varepsilon_F = 0.062/\eta - \eta^2$ , while near the BCS limit  $\eta \rightarrow -\infty$ ,  $\mu/\varepsilon_F = 1 + 0.707/\eta$ . Overall good agreement with Quantum Monte Carlo results is found.

## I. INTRODUCTION

BEC-BCS crossover is a field attracting lots of attention recently [1, 2, 3, 4, 5]. The simplest systems to study the crossover are dilute Fermion systems with attractive interactions, for which the effective range for two-body scattering is much less than the inter-particle spacing. At zero temperature, such systems are characterized by a dimensionless number  $\eta = 1/(ak_F)$ , where  $a$  is the two-body scattering length, and  $k_F$  is the corresponding Fermi momentum in non-interacting systems. For  $\eta$  large and negative (weak attraction) one finds the BCS solution with pairing and superfluidity. With  $\eta$  large and positive, corresponding to strong attraction with a two-body bound state well below threshold, the bound pairs will Bose-Einstein condense (BEC). Experimentally,  $\eta$  can be changed between the BEC and BCS limits at will using the technique of Feshbach resonance [6, 7, 8, 9, 10, 11, 12]. Theoretically, physical quantities are expected to be a smooth function of  $\eta$ , since there is no phase transition between the BEC and BCS limits. In each of these limits the behavior is nonperturbative, however, the effective interaction is weak; the system can be successfully described in a mean field approximation. On the other hand, dilute fermion systems near the unitarity limit (the  $\eta = 0$  limit) require treatments beyond the mean field approximation such as numerical simulations [13, 14, 15, 16, 17, 18, 19].

Recently, Nishida and Son have proposed an analytical approach called “ $\epsilon$  expansion” to deal with problems near the unitarity limit [20, 21]. In this approach one computes physical quantities in  $d$  spacial dimensions, then treats  $\epsilon = 4 - d$  as a small expansion parameter, and then sets  $\epsilon = 1$  at the end to obtain the three dimensional physics. It is similar to the dimensional expansion method used by Wilson to study critical exponents of second order phase transitions [22]. Nishida and Son’s idea was inspired by the observation of Nussinov and Nussinov [23] that the ground state of a two-component fermion system in the unitarity limit is a free Bose gas for  $d \geq 4$  (also see Refs. [24, 25] for simplification of certain diagrams with  $d \rightarrow \infty$ ). It is because the two Fermion bound state (with zero binding energy) wave function behaves as  $\Phi(r) \propto 1/r^{d-2}$ , where  $r$  is the separation between the two Fermions. The probability integral  $\int d^d r |\Phi(r)|^2$  has a singularity at  $r \rightarrow 0$  when  $d \geq 4$ . Thus the bound state has zero size and will not interact with each other. This feature was explicitly implemented in the theory set up near the unitarity limit in Refs. [20, 21]. As we will see, away from the unitarity limit, one also expects the localization of the bound state wave function all the way to the BEC limit but not to the BCS limit.

Now the  $\epsilon$  expansion has been applied to few-body scattering [26], polarized fermions (i.e., with uneven chemical potential between two fermion species) in the unitarity limit [27], and near the unitarity limit [21] to identify the “splitting point” in the phase diagram where three different phases meet [28]. The critical temperature in the unitarity limit has also been computed [29]. Recently, the first next-to-next-to-leading order (NNLO) calculation in the  $\epsilon$  expansion was carried out for  $\mu/\varepsilon_F$  in the unitarity limit, where  $\mu$  is the Fermion chemical potential and  $\varepsilon_F$  is the Fermi energy in non-interacting systems [30]. Contrary to the nice convergence seen previously at next-to-leading order (NLO), the NNLO of  $\mu/\varepsilon_F$  is as large as the leading order (LO) with an opposite sign. Even so, it is still premature to claim that the large NNLO correction cannot be tamed through reorganizing the series. Thus, we consider it is still worth while to explore the  $\epsilon$  expansion at lower orders.

In this work, we apply the  $\epsilon$  expansion to NLO to study the BEC-BCS transition with an arbitrary  $\eta$ . In the BEC side, an interesting relation between  $\mu$  and the two fermion binding energy  $B$  is implemented:

$$2\mu + B = \mathcal{O}(\epsilon). \quad (1)$$

This comes from the chemical equilibrium between two fermions (with chemical potential  $2\mu$ ) and one boson (with chemical potential  $-B$ ) in a 4-d system where the bosons do not interact with each other. We also perform the resummation of the  $(\epsilon \log \eta)^n / n!$  terms arising from  $\eta^\epsilon - 1$ . These logarithms are formally higher order in  $\epsilon$  but numerically important near the unitarity limit ( $\epsilon = 1$ ,  $|\eta| \ll 1$ ), and near the BEC and BCS limits ( $\epsilon = 1$ ,  $|\eta| \gg 1$ ). For example, this resummation gives the linear term in  $\mu/\epsilon_F$  when  $|\eta| \ll 1$ :

$$\frac{\mu}{\epsilon_F} = 0.475 - 0.707\eta - 0.5\eta^2. \quad (2)$$

Without this resummation, physical quantities are always even in  $\eta$  which would prevent us from reaching the BCS side.

## II. $\epsilon$ EXPANSION

We are interested in a two-component Fermi gas with zero range attractive interactions characterized by the scattering length  $a$ . In Nambu-Gor'kov formalism, the two-component fermions are denoted as  $\Psi = (\psi_\uparrow, \psi_\downarrow)^T$ . After the Hubbard-Stratonovich transformation, the Lagrangian of the system is

$$L = \Psi^\dagger \left( i\partial_t + \frac{\nabla^2}{2m} \sigma_3 + \mu \sigma_3 \right) \Psi + \Psi^\dagger \sigma_+ \Psi \phi + \Psi^\dagger \sigma_- \Psi \phi^* - \frac{\phi^* \phi}{c_0}, \quad (3)$$

where  $m$  is the fermion mass,  $\sigma_i$  is the Pauli matrix acting on the spin space, and the coupling  $c_0$  depends on the two-body scattering length  $a$ . The ground state is a superfluid state with a condensate  $\langle \phi \rangle = \phi_0$ , whose phase is chosen to be zero.  $\phi$  is then expanded around  $\phi_0$ ,

$$\phi = \phi_0 + g\varphi. \quad (4)$$

The Lagrangian will be further decomposed into perturbative and non-perturbative parts. We will first look at the BEC side, than the BCS side.

### A. Power Counting in the BEC Side

The Lagrangian can be decomposed as  $L = L_0 + L_1 + L_2$ ,

$$\begin{aligned} L_0 &= \Psi^\dagger \left[ i\partial_t + \left( \frac{\nabla^2}{2m} - \frac{B}{2} \right) \sigma_3 + \phi_0 \sigma_+ + \phi_0 \sigma_- \right] \Psi + \varphi^* \left( i\partial_t + \frac{\nabla^2}{4m} \right) \varphi - \frac{\phi_0^2}{c_0}, \\ L_1 &= \frac{\mu_B}{2} \Psi^\dagger \sigma_3 \Psi + g \Psi^\dagger \sigma_+ \Psi \varphi + g \Psi^\dagger \sigma_- \Psi \varphi^* + \mu_B \varphi^* \varphi, \\ L_2 &= -\varphi^* \left( i\partial_t + \frac{\nabla^2}{4m} + \frac{g^2}{c_0} \right) \varphi - \mu_B \varphi^* \varphi - g \frac{\phi_0}{c_0} (\varphi^* + \varphi), \end{aligned} \quad (5)$$

with  $B = 1/(ma^2)$ .  $\mu_B = 2\mu + B \sim \mathcal{O}(\epsilon)$  from Eq. (1) which will be checked explicitly later. Near the BEC limit ( $\eta \gg 1$ ),  $B$  does not vanish in 4-d, thus  $B \sim \mathcal{O}(\epsilon^0)$  and  $\mu = (\mu_B - B)/2 \sim \mathcal{O}(\epsilon^0)$ . Similarly,  $\phi_0$  does not vanish in 4-d in the BEC side. So  $\phi_0 \sim \mathcal{O}(\epsilon^0)$ .  $c_0$  is determined by demanding the two fermion scattering amplitude has a  $1/(p - i/a)$  pole in momentum  $p$  in arbitrary dimensions [26]:

$$\frac{1}{c_0} = \frac{m}{(4\pi)^{2-\epsilon/2} a^{2-\epsilon}} \Gamma\left(-1 + \frac{\epsilon}{2}\right). \quad (6)$$

In 3-d ( $\epsilon = 1$ ),  $1/c_0 = -m/(4\pi a)$  where  $a$  could be either positive (in the BEC side) or negative (in the BCS side). However in 4-d ( $\epsilon = 0$ ), the scattering amplitude has a double pole  $1/(p^2 + 1/a^2)$ . Thus, the sign of  $a$  does not play a role in 4-d and the difference between the BEC and BCS sides becomes

ambiguous. Besides, if  $a < 0$ ,  $1/c_0$  picks up a phase when  $0 < \epsilon < 1$ . To fix this phase, instead of using Eq. (6), we will use

$$\frac{1}{c_0} = \text{sign}[a] \frac{m}{(4\pi)^{2-\epsilon/2} |a|^{2-\epsilon}} \Gamma\left(-1 + \frac{\epsilon}{2}\right), \quad (7)$$

and write the  $|a|$  dependence in  $1/c_0$  as

$$\begin{aligned} |a|^{-2+\epsilon} &= a^{-2} (1 + \epsilon X), \\ X &= (|a|^\epsilon - 1)/\epsilon = \sum_{n=1}^{\infty} \frac{(\epsilon \log |a|)^n}{\epsilon n!}, \end{aligned} \quad (8)$$

such that all the higher order logarithms are resummed and lumped into NLO. Then  $|a|^{-2+\epsilon} \rightarrow 1/|a|$  at NLO after  $\epsilon \rightarrow 1$  is taken at the end. Using this prescription,  $1/c_0 \sim \mathcal{O}(\epsilon^{-1})$ .

$L_0$  is the non-perturbative part of the lagrangian which defines the fermion and boson propagators,

$$S_F(p, B) = \frac{-1}{\{p_0(1+i0^+)\}^2 - E_p^2} \begin{bmatrix} p_0 + \varepsilon_p + B/2 & -\phi_0 \\ -\phi_0 & p_0 - \varepsilon_p - B/2 \end{bmatrix}, \quad (9)$$

$$D(p) = \frac{-1}{p_0(1+i0^+) - \varepsilon_p/2}, \quad (10)$$

where  $\varepsilon_p = \mathbf{p}^2/(2m)$ ,  $E_p^2 = (\varepsilon_p + B/2)^2 + \phi_0^2$  and  $B/2$  plays the role of effective mass for the fermions.  $L_1$  gives the perturbative interaction with  $g \sim \mathcal{O}(\epsilon^{1/2})$  and  $\mu_B \sim \mathcal{O}(\epsilon^1)$ , while  $L_2$  gives the counterterms for boson self energy and tadpole diagrams. The boson-fermion coupling  $g$  is tuned to

$$g = \frac{\sqrt{8\pi^2\epsilon}}{m} \left(\frac{m\phi_0}{2\pi}\right)^{\epsilon/4} \sim \mathcal{O}(\epsilon^{1/2}), \quad (11)$$

such that the boson self energy diagram without(with) an insertion of  $\mu_B$  will be canceled by the first(second) term in  $L_2$  in 4-d. The last term in  $L_2$  cancels the leading boson tadpole diagram when  $\phi_0$  is chosen to minimize its effective potential.

The quantity we will compute in this paper is  $\mu/\varepsilon_F$ . Following the procedure of Ref. [20], we first compute the effective potential  $V_{\text{eff}}(\phi_0)$  and find the solution  $\bar{\phi}_0$  that minimizes  $V_{\text{eff}}$ . From  $V_{\text{eff}}$ , the fermion number density is

$$n_f = - \left. \frac{\partial V_{\text{eff}}}{\partial \mu} \right|_{\phi_0 = \bar{\phi}_0}. \quad (12)$$

Then  $\varepsilon_F$  is

$$\varepsilon_F = \frac{2\pi}{m} \left[ \frac{1}{2} \Gamma\left(3 - \frac{\epsilon}{2}\right) n_f \right]^{\frac{2}{4-\epsilon}}. \quad (13)$$

The leading diagrams for the effective potential  $V_{\text{eff}}(\phi_0)$  are listed in Fig. 1.

The tree level diagram in Fig. 1(a) gives a contribution

$$V_{c_0}(\phi_0) = \frac{\phi_0^2}{c_0} = \frac{B}{2^{2-\frac{\epsilon}{2}}} \Gamma\left(-1 + \frac{\epsilon}{2}\right) [\epsilon Q(\phi_0) + 1] \left(\frac{\phi_0 m}{2\pi}\right)^{2-\epsilon/2} \sim \mathcal{O}(\epsilon^{-1}), \quad (14)$$

where

$$Q(\phi_0) = \frac{1}{\epsilon} \left[ \text{sign}[a] \left(\frac{\phi_0}{B}\right)^{\epsilon/2} - 1 \right] \sim \mathcal{O}(\epsilon^0). \quad (15)$$

The one-loop diagram in Fig. 1(b) yields

$$\begin{aligned} V_{1L}(\phi_0) &= - \int \frac{d^5 p}{i(2\pi)^{5-\epsilon}} \ln \det [S_F^{-1}(p, B)] \\ &= \phi_0 \left(\frac{\phi_0 m}{2\pi}\right)^{\frac{4-\epsilon}{2}} \frac{\pi \left(\frac{B}{\phi_0}\right)^{1-\epsilon/2} {}_2F_1\left(\frac{-2+\epsilon}{4}, \frac{\epsilon}{4}; 2; \frac{-4\phi_0^2}{B^2}\right)}{2^{2-\epsilon/2} \sin\left(\frac{\pi\epsilon}{2}\right) \Gamma(2-\epsilon/2)} \\ &\sim \mathcal{O}(\epsilon^{-1}), \end{aligned} \quad (16)$$

$$\sim \mathcal{O}(\epsilon^{-1}), \quad (17)$$

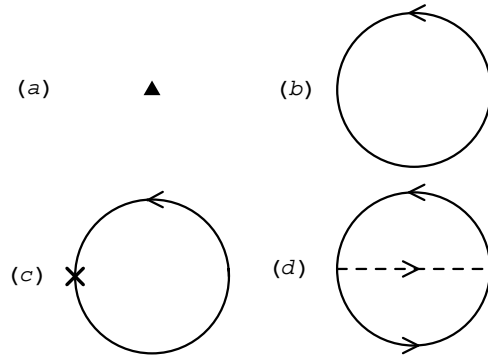


FIG. 1: Feynman diagrams for the  $\phi_0$  effective potential up to  $\mathcal{O}(\epsilon)$ . The solid triangle is the  $\phi_0^2/c_0$  potential. The solid lines are fermion propagators and dashed lines are boson propagators. The cross denotes one insertion of  $\mu_B$ .

where  ${}_2F_1$  is a hypergeometric function. The one-loop diagram in Fig. 1(c) with one insertion of  $\mu_B$  yields

$$V_{1L\mu_B}(\phi_0) = -\mu_B \frac{\partial V_{1L}(\phi_0)}{\partial B} \sim \mathcal{O}(1). \quad (18)$$

Also, the two-loop diagram in Fig. 1(d) yields

$$\begin{aligned} V_{2L}(\phi_0) &= g^2 \int \frac{dp^{5-\epsilon} dq^{5-\epsilon}}{i(2\pi)^{5-\epsilon} i(2\pi)^{5-\epsilon}} \text{Tr} [S_F(p, B)\sigma_+ S_F(q, B)\sigma_-] D(p-q) \\ &= -\tilde{C}(B/\phi_0) \epsilon \phi_0 \left( \frac{\phi_0 m}{2\pi} \right)^{\frac{4-\epsilon}{2}} \\ &\sim \mathcal{O}(\epsilon), \end{aligned} \quad (19)$$

where  $\tilde{C}(z)$  is a decreasing function of  $z$  which converges numerically even at 4-d. The expression for  $\tilde{C}(z)$  and its numerical plot are shown in the Appendix. So now we have

$$V_{\text{eff}} = V_{c_0} + V_{1L} + V_{1L\mu_B} + V_{2L}. \quad (20)$$

### B. Near the Unitarity Limit

Now we study  $\mu/\varepsilon_F$  near the unitary limit by small  $B$  expansion of  $V_{\text{eff}}$  to  $\mathcal{O}(B)$ . The  $\mathcal{O}(\epsilon^{-1})$  contributions cancel as

$$-V_{c_0}(\phi_0) = V_{1L}(\phi_0) = \frac{m^2 \phi_0^2}{8\pi^2 \epsilon} B + \mathcal{O}(\epsilon^0). \quad (21)$$

The resulting  $\bar{\phi}_0$  that minimizes  $V_{\text{eff}}$  is

$$\begin{aligned} \bar{\phi}_0 &= \frac{\mu_B}{\epsilon} + \frac{B}{2} (2Q(\bar{\phi}_0) + 1) \\ &+ \left[ \frac{\mu_B}{\epsilon} (3C_1 + \ln 2 - 1) + B \left\{ C_2 + \left( 3C_1 + \ln 2 - \frac{1}{2} \right) \left( Q(\bar{\phi}_0) + \frac{1}{2} \right) - \frac{1}{4} + \frac{\pi^2}{48} \right\} \right] \epsilon + \mathcal{O}(\epsilon^2), \end{aligned} \quad (22)$$

where  $C_1 = \tilde{C}(0) = 0.1442$  [20] and  $C_2 = \tilde{C}'(0) = -0.223$  arise from  $V_{2L}(\phi_0)$  with

$$V_{2L}(\phi_0) = -\epsilon \left( C_1 \phi_0 + C_2 \frac{B}{2} \right) \left( \frac{\phi_0 m}{2\pi} \right)^{\frac{4-\epsilon}{2}} + \mathcal{O}(\epsilon^2). \quad (23)$$

Since  $\bar{\phi}_0 \sim \mathcal{O}(\epsilon^0)$ , Eq. (22) shows that  $\mu_B$  should be  $\mathcal{O}(\epsilon)$ , which agrees with the intuitive argument given above.

Next, we obtain  $\varepsilon_F$  as a function of  $\mu_B$ :

$$\frac{\mu_B}{\varepsilon_F} = -\frac{B}{2\varepsilon_F} (2Q(\bar{\phi}_0) + 1) + \epsilon^{1/2} - \frac{B}{\varepsilon_F} \left( C_2 + \frac{Q(\bar{\phi}_0)}{2} + \frac{\pi^2}{48} - \frac{1}{4} \right) \epsilon + \mathcal{O}(\epsilon^{5/2}). \quad (24)$$

By taking the LO of  $\bar{\phi}_0$  in Eq. (22) and substituting  $\mu_B$  by the LO expression in Eq. (24), one obtains  $\bar{\phi}_0 = \varepsilon_F \epsilon^{1/2} + \mathcal{O}(\epsilon)$  which implies  $\varepsilon_F \sim \mathcal{O}(\epsilon^{-1/2})$ .  $\bar{\phi}_0$  can further be solved to higher orders in  $\epsilon$  by interaction. Finally, we obtain

$$\begin{aligned} \frac{\mu}{\varepsilon_F} &= \frac{\epsilon^{3/2}}{2} \left[ 1 + \frac{\epsilon \ln \epsilon}{8} + \frac{5(1 - \ln 2) - 12C_1}{4} \epsilon \right] - \frac{1}{2} \left[ \text{sign}[a] \left( \frac{B}{\varepsilon_F \epsilon^{1/2}} \right)^{-\epsilon/2} + \frac{\epsilon}{2} \right] \frac{B}{\varepsilon_F} + \mathcal{O}(\epsilon^{7/2}, B\epsilon^{5/2}) \\ &\rightarrow 0.475 - 0.707\eta - 0.5\eta^2, \end{aligned} \quad (25)$$

where the arrow in the second line denotes extrapolation to three dimension  $\epsilon \rightarrow 1$ , and we have used  $B/\varepsilon_F = 2(ak_F)^{-2} = 2\eta^2$ . Note that the result of Ref. [21] is reproduced if we truncate the expansion of  $(B/\varepsilon_F \epsilon^{1/2})^{-\epsilon/2}$  as  $1 - \epsilon/2 \log[B/\varepsilon_F] + \epsilon/4 \log[\epsilon]$ , which does not give a linear term in  $\eta$ . In order to compare with the Quantum Monte Carlo (QMC) results [13, 14],  $\mu/\varepsilon_F$  can be converted to energy per particle relative to the value of a non-interacting fermi gas

$$\xi = \frac{E/A}{E_0/A} \quad (26)$$

with  $E_0/A = 3/5\varepsilon_F$  in 3-d. The relation is,  $\mu/\varepsilon_F = \xi - \frac{\eta}{5} \frac{\partial \xi}{\partial \eta}$ . Our result gives  $\xi \simeq 0.475 - 0.884\eta - 0.833\eta^2$ . This is compared with two sets of QMC results denoted as QMC1[13] and QMC2 [14] in Fig. 2.

### C. The BEC Limit

In BEC limit,  $B \gg \varepsilon_F$  or  $\eta \gg 1$ , we perform  $1/B$  expansion to  $\mathcal{O}(B^{-2})$ . Note that  $V_{2L}(\phi_0) \sim \mathcal{O}(B^{-2})$  and is neglected. The effective potential has a simple expression

$$V_{\text{eff}}(\phi_0) = \frac{2^{\epsilon-8} m^2 \pi^{\epsilon/2-1} \phi_0^2 (\epsilon \phi_0^2 - 16B\mu_B)}{B(Bm)^{\epsilon/2} \sin(\frac{\pi\epsilon}{2}) \Gamma(1 - \frac{\epsilon}{2})} + \mathcal{O}(B^{-2}), \quad (27)$$

which is minimized when  $\phi_0 = \bar{\phi}_0 = 2\sqrt{2B\mu_B/\epsilon}$ . Following the same procedure, we obtain

$$\begin{aligned} \frac{\mu}{\varepsilon_F} &= -\frac{B}{2\varepsilon_F} + \frac{\epsilon^2}{16} \left( 1 + \frac{3 - \ln 4}{4} \epsilon \right) \left( \frac{B}{\varepsilon_F} \right)^{\epsilon/2-1} \\ &\rightarrow 0.062\eta^{-1} - \eta^2. \end{aligned} \quad (28)$$

This result is corresponding to  $\xi = 0.052\eta^{-1} - \frac{5}{3}\eta^2$ . Note that the  $\eta^2$  term just comes from the free molecule contributions, while the  $\eta^{-1}$  correction is from the  $\phi_0^4$  term in  $V_{\text{eff}}$ , corresponding to the mean boson-boson interaction. The numerical value agrees well with the QMC1 result, which yields  $\xi = 0.055\eta^{-1} - \frac{5}{3}\eta^2$  [14]. The QMC2 calculation used a finite range cosh shape potential, thus the deviation from the QMC1 curve indicate the finite range effects.

### D. Power Counting in the BCS Side

Next we will turn to the BCS limit,  $-\eta \gg 1$ , where the situation changes drastically. As  $-a \rightarrow 0$ , the gap vanishes and the ground state should be a non-interacting Fermion gas with  $\Delta \equiv \bar{\phi}_0/\mu \ll 1$ . Thus we will count  $\mu$  to be  $\mathcal{O}(\epsilon^0)$ . And since Eq. (1) is no longer valid, we will write the Lagrangian as  $L = L_0 + L_1 + L_2$ , where

$$\begin{aligned} L_0 &= \Psi^\dagger \left[ i\partial_t + \left( \frac{\nabla^2}{2m} + \mu \right) \sigma_3 + \phi_0 \sigma_+ + \phi_0 \sigma_- \right] \Psi + \varphi^* \left( i\partial_t + \frac{\nabla^2}{4m} + 2\mu - \frac{g^2}{c_0} \right) \varphi - \frac{\phi_0^2}{c_0}, \\ L_1 &= g\Psi^\dagger \sigma_+ \Psi \varphi + g\Psi^\dagger \sigma_- \Psi \varphi^*, \\ L_2 &= -\varphi^* \left( i\partial_t + \frac{\nabla^2}{4m} + 2\mu \right) \varphi - g\frac{\phi_0}{c_0} (\varphi^* + \varphi). \end{aligned} \quad (29)$$

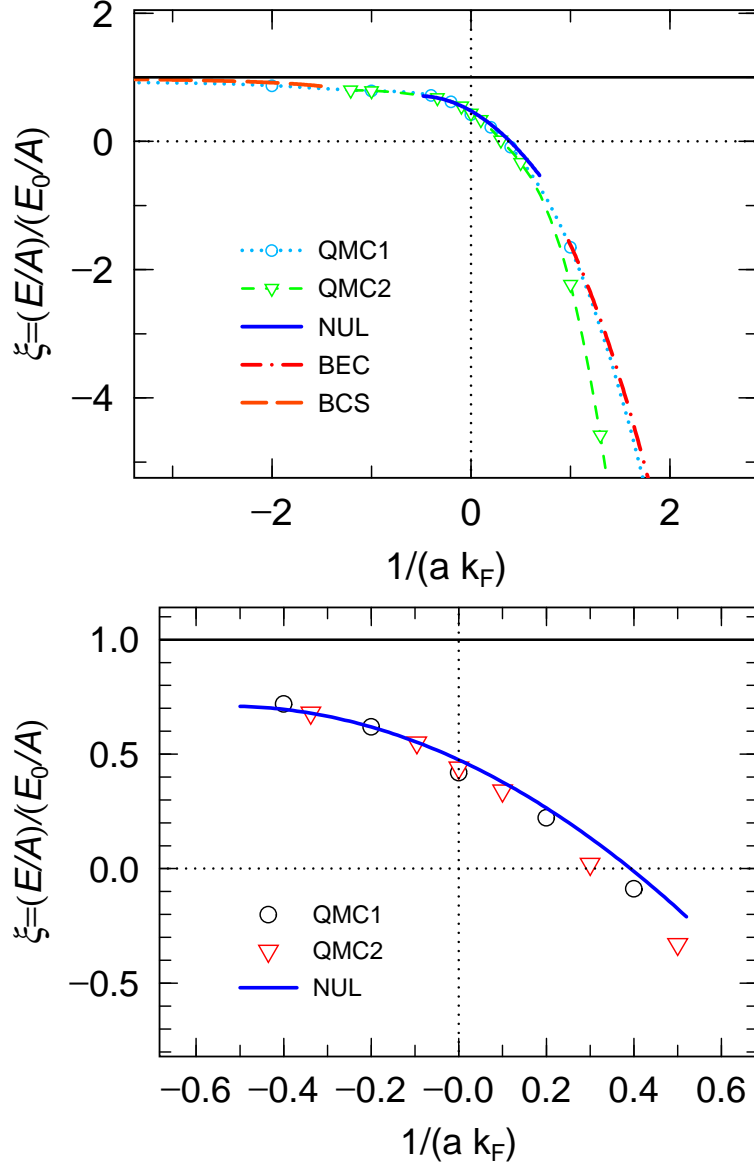


FIG. 2: (Color online)  $\xi$  (energy per particle relative to the value of a non-interacting fermi gas) shown as functions of  $(ak_F)^{-1}$ . QMC1 [13] and QMC2 [14] are Quantum Monte Carlo calculations with zero and finite range, respectively. NUL is our near unitarity limit result of Eq. (25) in the  $\epsilon$  expansion. BEC is our result in Eq. (28). BCS is obtained from numerical solving Eq. (36). The lower panel is the blow-up of the near unitarity regime.

In  $L_0$  the boson has an “effective mass”  $g^2/c_0 = B + \mathcal{O}(\epsilon)$  which will suppress the boson propagation in the BCS limit where  $B = 1/ma^2$  is big. Again, the boson self-energy renormalization vanishes at 4-d. The effective potential receives leading contributions from Fig. 1(a), (b), and (d) and yields

$$\begin{aligned}
 V_{\text{eff}}(\phi_0) = & V_{c_0}(\phi_0) - \int \frac{dp^{5-\epsilon}}{i(2\pi)^{5-\epsilon}} \ln \det [S_F^{-1}(p, -2\mu)] \\
 & + g^2 \int \frac{dp^{5-\epsilon} dq^{5-\epsilon}}{i(2\pi)^{5-\epsilon} i(2\pi)^{5-\epsilon}} \text{Tr} [S_F(p, -2\mu)\sigma_+ S_F(q, -2\mu)\sigma_-] \tilde{D}(p-q), \quad (30)
 \end{aligned}$$

where  $S_F(p, -2\mu)$  is the one defined in Eq.(9) with the substitution  $B \rightarrow -2\mu$ . The boson propagator  $\tilde{D}^{-1}(p) = -p_0(1 + i\delta) + \varepsilon_p/2 + B - 2\mu$  has been replaced by  $\tilde{D}^{-1}(p) = B$  which is a good approximation

when  $B \gg 2\mu$  or equivalently  $-\eta \gg 1$ . Since we expect  $\Delta \ll 1$ , by expanding to  $\mathcal{O}(\Delta^2)$  we obtain

$$\begin{aligned} \frac{V_{\text{eff}}}{m^{2-\epsilon/2}\mu^{3-\epsilon/2}} &= -\frac{1}{12\pi^2} \left[ 1 + \frac{\epsilon}{2} \left( 3\tilde{B}^{\epsilon/2-1} + \ln(2\pi) - \gamma + \frac{11}{6} \right) \right] + \frac{\Delta^2}{8\pi^2} \left[ \frac{\tilde{B}^{1-\epsilon/2} - 2}{\epsilon} \right. \\ &\quad \left. + \frac{1 - \gamma + \ln(4\pi)}{2} \tilde{B}^{1-\epsilon/2} + 2\tilde{B}^{\epsilon/2-1} + \gamma + \ln \frac{\Delta^2}{8\pi} \right], \end{aligned} \quad (31)$$

where  $\tilde{B} \equiv B/\mu$ .

At this order, the gap equation,  $\partial V_{\text{eff}}/\partial\Delta = 0$ , has a simple solution

$$\epsilon \ln \Delta = 1 - \frac{\tilde{B}^{1-\epsilon/2}}{2} - \epsilon \left( \frac{\ln(4\pi) - \gamma + 1}{4} \tilde{B} + \tilde{B}^{-1} + \frac{1 + \gamma - \ln(8\pi)}{2} \right) + \mathcal{O}(\epsilon^2, \Delta^2). \quad (32)$$

Thus,  $\ln \Delta \sim \mathcal{O}(\epsilon^{-1})$ . We will formally count  $\Delta \sim \mathcal{O}(\epsilon^{1/2})$  in Eq.(31) to indicate the smallness of the gap.

The  $n_f$  and  $\varepsilon_F$  can be computed using Eqs. (12) and (13):

$$\begin{aligned} \frac{\mu}{\varepsilon_F} &= 1 - \epsilon \tilde{B}^{\epsilon/2-1} - \frac{3\Delta^2}{2\epsilon} \left\{ 1 - \frac{\tilde{B}^{1-\epsilon/2}}{3} \right. \\ &\quad \left. + \epsilon \left[ \tilde{B} \left( \frac{6\gamma - 6\ln(8\pi) - 11}{72} \right) - \frac{7}{3} \tilde{B}^{-1} + \frac{1 - 2\gamma + 10\ln 2 + 2\ln \pi}{8} - \ln \Delta \right] \right\}. \end{aligned} \quad (33)$$

Since  $\tilde{B} = \frac{2}{(ak_F)^2} \frac{\varepsilon_F}{\mu}$  and  $\mu/\varepsilon_F = 1 + \mathcal{O}(\epsilon^0)$ , Eq. (32) shows that

$$\Delta \simeq \exp \left[ \frac{1 - |ak_F|^{-2+\epsilon}}{\epsilon} \right]. \quad (34)$$

This implies that, in 4-d, the gap vanishes and  $\mu/\varepsilon_F = 1$  when  $-ak_F \ll 1$ . In 3-d and with  $-ak_F \ll 1$ , the gap is exponentially suppressed. One might argue that  $\Delta$  should be smaller than  $\mathcal{O}(\epsilon^{1/2})$  as counted in Eq.(31). This is certainly true when  $\epsilon \rightarrow 0$ . However, since we will take  $\epsilon \rightarrow 1$  at the end, this counting suits our purpose especially when working between the BCS and unitarity limits.

To compare with the low energy theorem  $\xi = 1 + \frac{10}{9\pi}\eta^{-1} + \mathcal{O}(\eta^{-2})$  obtained in [31, 32], we perform a  $1/\eta$  expansion to Eq.(33). At NLO ( $\mathcal{O}(\epsilon)$ ) with all the exponentially suppressed  $\mathcal{O}(\Delta^2)$  terms neglected, we see no  $\eta^{-1}$  correction. However, we expect that at NNLO, the  $\epsilon\tilde{B}^{\epsilon/2-1}$  will be fully recovered and gives

$$\frac{\mu}{\varepsilon_F} \simeq 1 + \frac{ak_F}{\sqrt{2}}, \quad (35)$$

as  $\epsilon \rightarrow 1$ . This implies  $\xi = 1 + 0.589\eta^{-1} + \mathcal{O}(\eta^{-2}, \epsilon^2)$ . This agrees reasonably well with the low energy theorem.

As  $-\eta$  becomes smaller but not much smaller than unity, the  $\mathcal{O}(\Delta^2)$  effect in  $\mu/\varepsilon_F$  becomes more important. From the thermodynamic relation  $E/A = V_{\text{eff}}/n_f + \mu$ , we obtain

$$\begin{aligned} \xi &= 1 - \epsilon \frac{3}{4} \tilde{B}^{-1} \\ &\quad + \frac{1}{8} \left[ 27\tilde{B}^{-1} + [3\gamma - 3\ln(2\pi) - 4] \tilde{B} - 13 - 6\gamma + 6\ln(2\pi) \right] \Delta^2. \end{aligned} \quad (36)$$

Eqs. (32) and (36) give  $\xi$  in terms of  $\tilde{B}$ , while Eq.(33) gives  $\tilde{B}$  in terms of  $ak_F$ . The numerical result of  $\xi$  as a function of  $ak_F$  is shown as the BCS curve in Fig. 2.

### III. CONCLUSIONS

We have extended the  $\epsilon$  expansion (expansion around four spacial dimensions) developed by Nishida and Son for a cold fermi gas with infinite scattering length to finite scattering length to study the BEC-BCS crossover. A resummation of higher order logarithms and a suitable extension of fermion coupling

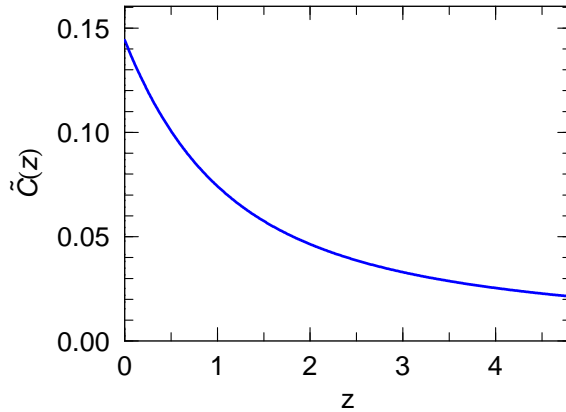


FIG. 3: The  $\tilde{C}(z)$  function that appears in Eq. (19)

in d-dimensions (see the discussion around Eqs. (7-8)) have been developed in order to apply the theory in the BCS regime. The ratio between the chemical potential and the Fermi energy,  $\mu/\varepsilon_F$ , has been computed to next-to-leading order in the  $\epsilon$  expansion as a function of  $\eta = 1/(ak_F)$ . Near the unitarity limit  $|\eta| \rightarrow 0$ , we found  $\mu/\varepsilon_F = 0.475 - 0.707\eta - 0.5\eta^2$ . Near the BEC limit  $\eta \rightarrow \infty$ ,  $\mu/\varepsilon_F = 0.062/\eta - \eta^2$ , and near the BCS limit  $\eta \rightarrow -\infty$ ,  $\mu/\varepsilon_F = 1 + 0.707/\eta$ . As shown in Fig. 2, overall good agreement with Quantum Monte Carlo results has been found.

#### IV. APPENDIX

The function  $\tilde{C}(z)$  that appears in Eq. (19) is defined as

$$\tilde{C}(z) = \int_{z/2}^{\infty} dx \int_{z/2}^{\infty} dy \frac{(\sqrt{x^2+1}-x)(\sqrt{y^2+1}-y)}{2\sqrt{x^2+1}\sqrt{y^2+1}} \times \left( -z + x + y + 2\sqrt{x^2+1} + 2\sqrt{y^2+1} - \sqrt{\left[ -z + x + y + 2(\sqrt{x^2+1} + \sqrt{y^2+1}) \right]^2 - (z-2x)(z-2y)} \right).$$

The numerical value of  $\tilde{C}(z)$  is plotted in Fig. 3.

In Eq.(30), the one fermion loop contribution to the effective potential near the BCS limit has the analytic expression:

$$- \int \frac{dp^{5-\epsilon}}{i(2\pi)^{5-\epsilon}} \ln \det [S_F^{-1}(p, -2\mu)] = \frac{2^{\frac{\epsilon}{2}-4} \pi^{\frac{\epsilon-5}{2}} \Delta^{2-\frac{\epsilon}{2}}}{\Gamma(2-\frac{\epsilon}{2})} \times \left[ \Delta \Gamma \left( 1 - \frac{\epsilon}{4} \right) \Gamma \left( \frac{\epsilon-6}{4} \right) {}_2F_1 \left( \frac{\epsilon-6}{4}, \frac{\epsilon-2}{4}; \frac{1}{2}; -\frac{1}{\Delta^2} \right) + 2\Gamma \left( \frac{3}{2} - \frac{\epsilon}{4} \right) \Gamma \left( \frac{\epsilon}{4} - 1 \right) {}_2F_1 \left( \frac{\epsilon}{4}, \frac{\epsilon}{4} - 1; \frac{3}{2}; -\frac{1}{\Delta^2} \right) \right]$$

#### V. ACKNOWLEDGEMENTS

We would like to thank Chung-Wen Kao for helpful discussion. This work was supported by the NSC and NCTS of Taiwan, ROC.

---

[1] A. J. Leggett, *Modern trends in the Theory of Condensed Matter*, Springer-verlag, Berlin (1980), p. 13.  
[2] P. Nozières and S. Schmitt-Rink, *J. Low Temp. Phys.* **59**, 195 (1985).



- [3] M. Randeria, *Bose-Einstein Condensation*, ed. A. Griffin, D. W. Snoke, and S. Stringari, Cambridge, N. Y., (1995), p. 355.
- [4] Y. Ohashi and A. Griffin, Phys. Rev. Lett. **89**, 130402 (2002) [cond-mat/0201262].
- [5] For a review, Q. Chen, J. Stajic, S. Tan, and K. Levin, Phys. Rep. **412**, 1 (2005).
- [6] K. M. O'Hara *et al.*, Science **298**, 2179 (2002).
- [7] C. A. Regal, M. Greiner, and D. S. Jin, Phys. Rev. Lett. **92**, 040403 (2004).
- [8] M. Bartenstein *et al.*, Phys. Rev. Lett. **92**, 120401 (2004).
- [9] M. W. Zwierlein *et al.*, Phys. Rev. Lett. **92**, 120403 (2004).
- [10] J. Kinast *et al.*, Phys. Rev. Lett. **92**, 150402 (2004).
- [11] T. Bourdel *et al.*, Phys. Rev. Lett. **93**, 050401 (2004).
- [12] J. Kinast *et al.*, Science **307**, 1296 (2005).
- [13] G. E. Astrakharchik, J. Boronat, J. Casulleras, and S. Giorgini, Phys. Rev. Lett. **93**, 200404 (2004) [cond-mat/0406113].
- [14] J. Carlson, S. Y. Chang, V. R. Pandharipande, and K. E. Schmidt, Phys. Rev. Lett. **91**, 050401 (2003); S. Y. Chang, V. R. Pandharipande, J. Carlson, and K. E. Schmidt, Phys. Rev. A **70**, 043602 (2004).
- [15] J. W. Chen and D. B. Kaplan, Phys. Rev. Lett. **92**, 257002 (2004).
- [16] M. Wingate, Nucl. Phys. Proc. Suppl. 140:592-594, 2005; cond-mat/0502372; hep-lat/0609054.
- [17] J. Carlson and S. Reddy, Phys. Rev. Lett. **95**, 060401 (2005) [cond-mat/0503256].
- [18] A. Bulgac, J. E. Drut, and P. Magierski, Phys. Rev. Lett. **96**, 090404 (2006).
- [19] D. Lee, Phys. Rev. B **73**: 115112 (2006); cond-mat/0606706; Phys. Rev. B **73**:115112 (2006); Phys. Rev. C **73**:015202 (2006).
- [20] Y. Nishida and D. T. Son, Phys. Rev. Lett. **97** [cond-mat/0604500].
- [21] Y. Nishida and D. T. Son, cond-mat/0607835.
- [22] K. G. Wilson and J. Kogut, Phys. Rep. **12**, 75 (1974).
- [23] Z. Nussinov and S. Nussinov, cond-mat/0410597.
- [24] J. V. Steele, nucl-th/0010066.
- [25] T. Schafer, C. W. Kao, and S. R. Cotanch, Nucl. Phys. A **762**, 82 (2005) [nucl-th/0504088].
- [26] G. Rupak, nucl-th/0605074.
- [27] G. Rupak, T. Schafer, and A. Kryjevski, e-Print Archive: cond-mat/0607834.
- [28] D. T. Son and M. A. Stephanov, e-Print Archive: cond-mat/0507586.
- [29] Y. Nishida, e-Print Archive: cond-mat/0608321.
- [30] P. Arnold, J. E. Drut, and D. T. Son, cond-mat/0608477.
- [31] K. Huang and C. N. Yang, Phys. Rev. **105**, 767 (1957).
- [32] T. D. Lee and C. N. Yang, Letter to editor, 1119 (1957).